DOI: 10.1002/chem.200500887

Trianglamines—Readily Prepared, Conformationally Flexible Inclusion-Forming Chiral Hexamines

Jacek Gawronski,* Krystyna Gawronska, Jakub Grajewski, Marcin Kwit, Agnieszka Plutecka, and Urszula Rychlewska*[a]

Dedicated to Prof. Mieczyslaw Makosza on the occasion of his 70th birthday

Abstract: Trianglamines, macrocyclic heteraphanes, were readily synthesised through a [3+3] cyclocondensation of (*R*,*R*)-1,2-diaminocyclohexane with terephthalaldehyde, followed by $NaBH_4$ reduction and N-alkylation. The macrocyclic ring shows a remarkable ability to change its conformation, as a consequence of rotation about the C–N bonds or nitrogen inversion due to protonation or N-alkylation, as revealed by circular dichroism spectra, computational modelling and X-ray diffraction analysis. The flexible natures of the trianglamine macrocycles allow ready accommodation of a variety of guest molecules to form crystalline inclusion complexes of highly diversified interpenetrating structures.

Keywords: amines · circular dichroism · conformation analysis · macrocycles · X-ray diffraction

Introduction

Large-ring, noncollapsible heterocycles (heteraphanes),[1] particularly those of chiral structure, are of considerable interest for their promising applications as ligands, organocatalysts and scaffolds for biomimetic and nanopatterning purposes.[2] Large-scale applications of macrocycles are frequently limited by their availability and cost. Despite many advances in synthesis, efficient one-step assembly of a macrocycle[3] still represents a formidable challenge in terms of the number of synthesis steps, reaction conditions, chemical yield and atom economy.

We recently introduced a facile method for a one-step construction of large chiral hexaimine macrocycles **I**, through [3+3] cyclocondensations between enantiomerically pure *trans*-1,2-diaminocyclohexane and terephthalic or isophthalic aldehydes.[4] This reversible reaction provides the macrocycles in high yields, under nontemplated conditions and at relatively high substrate concentrations (typically $0.4\,\text{M}\,\text{L}^{-1}$) in a variety of solvents and is evidently favoured over linear polymer formation both kinetically and thermodynamically. With terephthalaldehyde and racemic *trans*-1,2-diaminocyclohexane, a diastereoisomeric [3+3] cyclocondensation product could be obtained, differing in molecular symmetry (C_2) from those obtained from the enantiomerically pure *trans*-1,2-diaminocyclohexanes (D_3 symmetry).[5]

Subsequently, triangular hexaimines **I** (named trianglimines by Kuhnert[6]) have been obtained from many rigid aromatic 1,3- and 1,4-dialdehydes incorporating biphenyl,[7,8] terphenyl,[9] quaterphenyl,[10] 9,10-anthryl,[8] benzene ring substituted,[6,7,11] heterocyclic[7,10] and stilbene or divinylbenzene structural motifs.[9] In the case of aromatic 1,3-dialdehydes, [2+2] and [4+4] cyclocondensation may compete with [3+3] cyclocondensation, resulting in mixtures of products.[7,12,13]

Hexaimines such as **II**, obtained from aromatic 1,3-dialdehydes,[14] have vaselike structure[15] and hence bear the name calixsalens.[16] Their Robson-type metal complexes have been studied recently.[17]

Examples of related [3+3] triangular 30-membered macrocyclic hexaimines formed from 1,2-diaminobenzene derivatives and 2,3-dihydroxybenzene-1,4-dicarbaldehyde have recently been reported.[18a,19a,b] However, high yields in this reaction could only be achieved when lower concentration of the substrates ($0.04\,\text{M}\,\text{L}^{-1}$ in acetonitrile) and long reaction times (two weeks at room temperature) were applied. Even larger triangular macrocycles were recently obtained

[a] Prof. Dr. J. Gawronski, Dr. K. Gawronska, Dr. J. Grajewski, Dr. M. Kwit, A. Plutecka, Prof. Dr. U. Rychlewska
Department of Chemistry, A. Mickiewicz University
Grunwaldzka 6, 60780 Poznan (Poland)
Fax: (+48) 61-865-8008
E-mail: gawronsk@amu.edu.pl
urszular@amu.edu.pl

Supporting information for this article is available on the WWW under http://www.chemeurj.org/ or from the author.

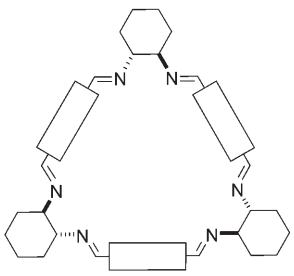

trianglimines
I

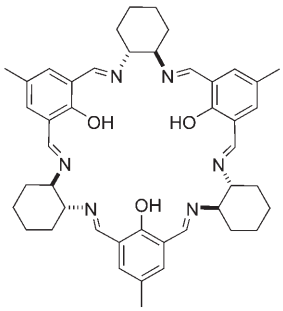

calixsalen
II

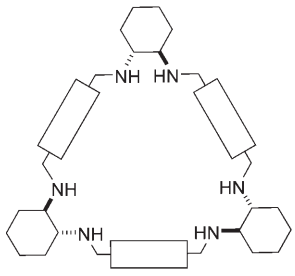

trianglamines
III

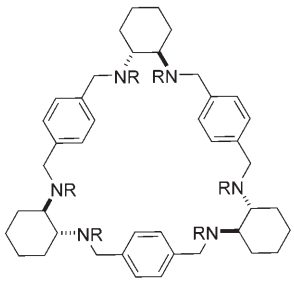

1-11

1: R = H
2: R = Me
3: R = $CH_2CH{=}CH_2$
4: R = $CH_2C{\equiv}CH$
5: R = CH_2CN
6: R = CH_2COOEt
7: R = CH_2CH_2OH
8: R = Bn
9: R = $CH_2C_6H_4$(4-Br)
10: R = $CH_2C_6H_4$(4-CN)
11: R = $CH_2C_6H_4$(4-OMe)

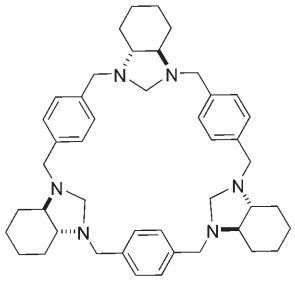

12

representative hexamines **1**, **2** and **12**, based on molecular modelling and circular dichroism (CD) spectra. Unusual inclusion complexes of **1** with aromatic compounds and their X-ray-determined structures, demonstrating conformational flexibility of **1** in the crystal state, are also reported.

Results and Discussion

Synthesis: A comparative study of the condensation of (*R*,*R*)-1,2-diaminocyclohexane and terephthalaldehyde in various solvents with subsequent $NaBH_4$ reduction in methanol was carried out: **1** was obtained in high yield and without noticeable amounts (ESI-MS) of the [2+2] cyclocondensation product in benzene, dichloromethane, tetrahydrofuran or acetonitrile. A small amount (below 3%) of the [2+2] cyclocondensation product was detected in the crude reaction product obtained in methanol. However, because of the convenience of carrying out the two-step synthesis in a one-pot fashion, methanol was chosen as a solvent in the synthesis of **1**.

The original[4] and the one-step[22] procedures for the preparation of trianglamine **1** were subsequently significantly improved. As a result, trianglamine **1** can now be prepared in 96–97% yield from the readily available (*R*,*R*)-tartrate salt of (*R*,*R*)-1,2-diaminocyclohexane,[24] rather than the more expensive free base, in a combination of the condensation with terephthalaldehyde and the sodium borohydride reduction of the intermediate trianglimine in a one-pot synthesis. We found that the reduction step can be carried out efficiently with less than half the amount of $NaBH_4$ used in a previous procedure[22] and that product **1** can be obtained as a free base, rather than as its hexahydrobromide salt. Eschweiler–Clark methylation of **1** afforded **2** in 71% yield. Attempted preparation of **2** by methylation at room temperature with methyl iodide in the presence of potassium carbonate resulted in a lower yield (ca. 50%) of the product.

Other N-alkylated trianglamines (**3**–**6** and **8**–**11**) were prepared by alkylation of **1** with the corresponding alkyl bromides in acetonitrile in the presence of potassium carbonate. Trianglamine **7** was obtained by $LiAlH_4$ reduction of **6**. It is of interest to note that, unlike other derivatives, hexakis(2-hydroxyethyl) derivative **7** shows significantly broadened ^1H NMR signals in $CDCl_3$ at room temperature, whereas a complex pattern of sharp signals is obtained on lowering the

from 1,2-diaminobenzene derivatives and hydroxylated aromatic dialdehydes.[18b,19c]

Successful [3+3] cyclocondensation requires that both substrates are predisposed[20] to perform the desired function; that is, both have rigid structures, with the diamine providing the apexes of the triangular product and the dialdehyde the sides. Indeed, with the use of the more conformationally flexible open-chain *syn*-1,2-diphenylethane-1,2-diamine the formation of oligomeric chain products was found to compete significantly with the cyclocondensation reaction.[6]

Trianglamines (**III**), products of reduction of trianglimines (**I**), are chiral hexamines.[4,7,8] The trianglamine derived from terephthalaldehyde and *trans*-1,2-diaminocyclohexane (**1**) has recently been used as a receptor for the recognition of aromatic tricarboxylic acids,[21] and the Zn^{II} complex of **1** was found to catalyse asymmetric aldol reactions.[22] Much better asymmetric induction in aldol and nitroaldol reactions was achieved with the use of a trinuclear—rather than mononuclear—Zn^{II} complex of the hexamine derived from calixsalen **II**.[23]

The structures and conformations of trianglimines[4,9,11] and calixsalens[15] have been analysed. Although the structures of trianglimines are in many cases shape-persistent, conformational analysis of trianglamine macrocycles represents a challenging task due to the anticipated ring flexibility: rotation of any of the ring single bonds can generate new stereostructures. In view of the significance and anticipated new applications of trianglamines we present here a one-step synthesis of trianglamine **1** and its N-derivatisation to provide **2**–**12**, together with a conformational analysis of

measurement temperature down to −50 °C. This suggests that the conformational equilibrium of **7** is strongly influenced by the formation of intramolecular hydrogen bonds within each of the β-aminoalcohol moieties. Broadened ^{1}H NMR signals are also observed at room temperature in the case of N-benzylated derivatives **8**–**11**.

Conformation and circular dichroism: Despite their formally high D_3 symmetry, trianglamines **1**–**12** represent a class of heteraphanes of considerable conformational diversity, due to low rotational barriers around the numerous single bonds. Attempts to compute low-energy conformers of the simplest representative **1**, with the MM3-CONFLEX routine, resulted in the generation of a large number of conformers belonging to families of qualitatively similar structures. A more rational approach, based on qualitative analysis of available conformers of **1**, was undertaken as shown below. In addition, we were fortunate enough to obtain quantitative structural data from X-ray analyses of crystal structures of the inclusion complexes of **1**, its hexahydrobromide salt and of **12** (see the following section). In order to reduce the number of variables (torsion angles) in the conformational analysis of **1** we made the following assumptions: 1) the cyclohexane rings are in chair conformations, with all carbon–nitrogen bonds equatorial, 2) the rotation of the 1,4-disubstituted benzene rings is not considered (in fact, rotational disorder of these rings is demonstrated even in the crystal structures; see below) and 3) only the rotation about the carbon–nitrogen bonds forming the macrocycle needs to be taken into account to define the macrocycle structure. This includes three sets of torsion angles—α, α', β and β'—for each trianglamine (see Figure 1).

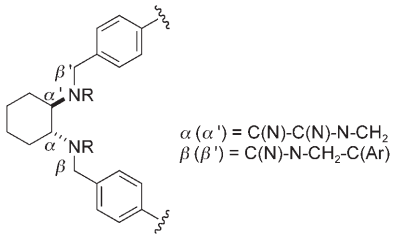

Figure 1. Definition of torsion angles α, α', β and β' involving flexible bonds in trianglimine **1** and its N-alkyl derivatives.

Each of the torsion angles shown in Figure 1 is initially restricted to either a gauche (G^-) or a *trans* (T) arrangement. Although this still gives rise to a large number of possible conformers of **1**, a further simplification can be obtained from the following consideration. The number of α, α', β or β' angles in *trans* (T) arrangements is unrestricted, as these give rise to expanded ring structures. G^- arrangements of α, α', β or β' produce folded-ring structures, such as those observed in the crystal state for a number of nonprotonated molecules of **1**, forming inclusion complexes with solvent guest molecules. The number of G^- bond arrangements in **1** is thus limited, as each G^- will produce additional ring folding (in the X-ray-determined structures there are no more than three G^- bond arrangements in the entire ring). Not available are macro ring structures in which both β and β' correspond to a G^- conformation, as the N–CH_2(Ar) bonds in such structures would assume orientations vertical to the average cyclohexane ring plane. No G^+ arrangement of α, α', β or β' is allowed in the (*R*,*R*)-1,2-diaminocyclohexane series, as such conformations would produce highly strained, ring-contracted structures (indeed, no such conformations are observed in the crystal structures). As a result of these restrictions, there are only a few sequences of torsion angles available for the macrocycle **1** (Table 1).

The data in Table 1 relate either to X-ray-determined structures or to the lowest-energy conformers obtained by structure optimisation by the MM3-AM1 protocol (see the Experimental Section). Note that the two calculated structures (**1** and **2**) contain anticlinal (A), rather than T, bond arrangements.

The conformers of **1** in solution give averaged NMR spectra at room temperature, but it was possible to elucidate the

Table 1. Sequences of torsion angles available for calculated and X-ray-determined structures of free and protonated trianglamines **1**, **2** and **12**, signs of the corresponding ^1B_a exciton Cotton effects generated by each pair of substituted benzene chromophores, and the distances between the chromophores.

	Sequences of torsion angles $\beta\alpha\alpha'\beta'$	Sign of exciton Cotton effect	Interchromophoric distances [Å][a]
1[b]	$TATG^-$	positive	6.42
	G^-TTT	positive	8.00
	G^-AG^-T	negative	7.24
1·PhF[c]	G^-TTT	positive	7.59
	$TTTG^-$	positive	7.26
	G^-TTT	positive	7.51
1·BzOMe[c]	$TTTG^-$	positive	7.34
	G^-TTT	positive	7.41
	TTG^-T	negative	7.37
1·AcOEt[c,d]	TG^-TG^-	positive	6.95
	G^-TTT	positive	7.09
	TTTT	negative	7.77
1·6 H^+[b]	TTTT	negative	8.39
	TTTT	negative	8.39
	TTTT	negative	8.39
1·6 HBr[c]	TTTT	negative	8.42
	TTTT	negative	8.46
	TTTT	negative	8.47
2[b]	TTTT	negative	7.92
	TG^-TT	negative	6.75
	TATT	negative	7.54
(R_N)-**2**·3 H^+[b]	TTTT	negative	8.07
	TTTT	negative	7.68
	$TTTG^-$	positive	7.73
12[b]	TTTT	negative	7.26
	TTTT	negative	7.26
	TTTT	negative	7.26
12·EtOH[c]	TTTT	negative	7.17
	TTTT	negative	7.05
	TTTT	negative	7.04

[a] Measured as the distance between the centres of the benzene rings. [b] Calculated lowest-energy conformer. [c] Found in the crystal structure. [d] Determined for *ent*-**1**·AcOEt.

dominant conformers of **1** in solution by CD spectroscopy. The diagnostic Cotton effects in the CD spectra of trianglimines are due to the ^1B_a-type transition in the 1,4-disubstituted benzene chromophores. This transition is polarised along the chromophore axis running through the 1,4-benzene carbon atoms. Note that the orientation of the ^1B_a electric dipole transition moments is independent of the rotation of the benzene rings. Orthogonal ^1B_b transitions cannot contribute significantly to the CD spectra, as the orientations of the transition dipoles are averaged through rotation of the benzene rings around the 1,4-carbon atom axes. Each of the $\beta\alpha\alpha'\beta'$ torsion angle sequences should generate exciton Cotton effects of differing sign and magnitude within the ^1B_a transition band in the CD spectrum below 200 nm (Table 1). Note that the distances between the benzene chromophores are much larger in conformers with all-T torsion angle sequences than in their G$^-$TTT or TG$^-$TT counterparts, so the (negative) CD contributions due to the all-T conformers are weaker. A positive CD couplet (absorbance (A) = 117, Table 2) within the strong ^1B_a absorption band at 191 nm

Table 2. Experimentally obtained CD/UV data (^1B_a transition region) for trianglamines **1**–**12**.

	CD $\Delta\varepsilon$ (λ in nm)	A	UV $\varepsilon\times10^{-3}$ (λ in nm)	Solvent[a]
1	62 (196) −55 (186)	117	138 (191)	A
2	−75 (198) 30 (189)	−105	153 (193)	C
3	60 (198) −30 (185)	90	142 (194)	A
4	53 (197) −16 (189)	69	145 (192)	A
5	40 (196) −40 (186)	80	120 (191)	A
6	107 (198) −64 (188)	171	136 (193)	A
7	150 (198) −118 (189)	268	120 (192)	A
8	180 (196) −290 (183)	470	337 (191)	C
9	292 (201) −262 (187)	554	327 (196)	C
10	216 (198) −234 (185)	450	284 (195)	A
11	298 (200) −290 (185)	588	326 (195)	A
12	−58 (199)	−58	156 (192)	A

[a] A = acetonitrile, C = cyclohexane.

(extinction coefficient (ε) = 138000) is recorded for **1** in acetonitrile. The intensity of the ^1B_a Cotton effects is significantly reduced on acidification with excess methanesulfonic acid (Figure 2). CD titration of **1** with aqueous methanesulfonic or hydrochloric acid has shown that the intensity of the ^1B_a Cotton effects is reduced only after addition of more than three equivalents of the acid.

We had previously observed a significant effect of amine protonation on the CD spectra, reflecting the amine conformational change.[25] This effect can be regarded as interconversion of the two chiral forms in response to pH change (molecular switch).[26] The results presented here can be interpreted as indicative of the equilibrium between the conformers containing $\beta\alpha\alpha'\beta'$ torsion angle sequences contributing to either positive or negative rotational strength. For nonprotonated trianglimine **1**, conformers generating positive Cotton effects dominate. On protonation with up to three equivalents of the acid these conformers still dominate, demonstrating the stabilising nature of the intramolecular hydrogen bond N···H–N. In fully protonated **1** the contribution due to the TTTT bond arrangement increases and a less intense positive exciton Cotton effect is observed.

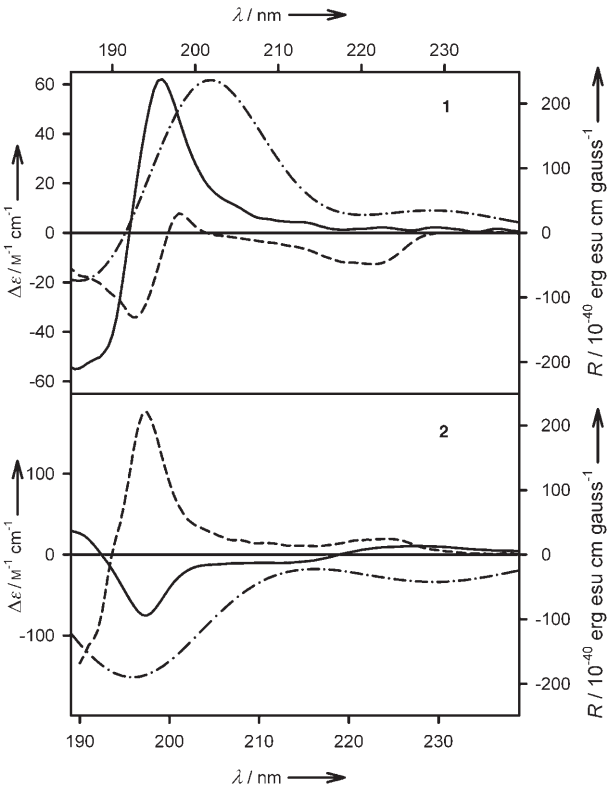

Figure 2. CD spectra of trianglamines **1** (upper panel) and **2** (lower panel): in acetonitrile (——), in acetonitrile with added approximately 60 equivalents of $MeSO_3H$ (-----), and calculated ZINDO/S CD spectra (–•–•) of the most stable conformers of **1** (upper panel) and **2** (lower panel). Rotational strength R is calculated in the dipole-length representation.

The conformation of the hexamethyl derivative **2** is of special interest as its ^1B_a Cotton effect is negative (Table 2, Figure 2). There is no intramolecular hydrogen bond between the nitrogen atoms in **2**, and the CD contribution due to conformers TTTT or TG$^-$TT appears to dominate. Note that in the TT conformer of **2** (Scheme 1) the methyl groups can either assume a vertical position (**A**) or, due to the rapid configuration inversion at nitrogen, one of them may be placed between the vicinal nitrogen atoms (**B**). On full protonation, hexamine **2** generates a very strong exciton Cotton effect of reverse (positive) sign (Figure 2). This indicates a dramatic change of conformation in the macrocycle

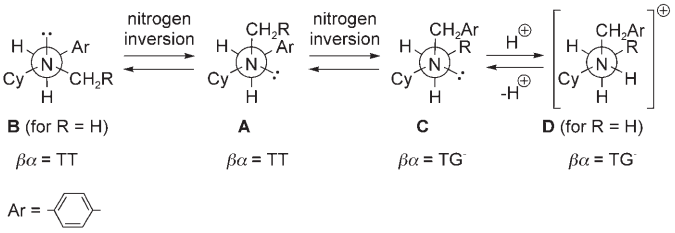

Scheme 1. Conformational changes of trianglamines involving configuration inversion at the nitrogen atom and protonation.

towards the folded structure, such as that represented by **D** in Scheme 1.

Computational modelling for **1** and **1**·6H$^+$ yielded low-energy conformers similar to those determined by X-ray diffraction analysis either for **1**·PhF or for **1**·PhCOOMe and **1**·6HBr, respectively (see Table 1). ZINDO/S-computed CD spectra for the calculated lowest-energy conformer of **1** are shown in Figure 2. Although we note a good agreement between the experimentally measured and the calculated CD curves for **1**, this is not the case for the fully protonated **1** (see the Supporting Information).

The computed lowest-energy structure for **2** (Table 1) is of the all-T type, with the exception of the two α angles in either G$^-$ or anticlinal (A) arrangements. As in the case of **1**, there is satisfactory agreement between the calculated and experimentally measured ^1B_a Cotton effects for **2** (Figure 2), but not for its protonated form. In fact, calculations for fully protonated **2** suggest that in one of the cyclohexane rings the C–N bonds are axial to produce a low-energy conformer. No axial C–N bonds are present, on the other hand, in the computed low-energy conformer of **2**·3H$^+$, in which every second nitrogen atom is protonated (C_3 symmetry). The computed structure of **2**·3H$^+$ (Table 1) is of all-T type, with the exception of one G$^-$ arrangement of angle β. The methyl groups occupy positions vertical to the macrocycle plane and all protonated nitrogen atoms have *R* configurations. The calculated ^1B_a Cotton effect for this structure (see the Supporting Information) is positive, in agreement with the experimental data (Figure 2).

Of further interest is the finding that trianglamines **3**–**11**, with substituents larger than the methyl group on the nitrogen atoms, all display positive exciton Cotton effects, with amplitudes varying according to the substituent. Inspection of Scheme 1 shows that the two nitrogen substituents of similar size, $-CH_2Ar$ (in the ring) and $-CH_2R$, can easily be exchanged by a nitrogen atom inversion process, resulting in the generation of conformer **C**. The very large Cotton effects of **8**–**11** are evidently due to contributions to the CD spectra from the chromophoric benzyl-type substituents at the nitrogen atoms.

Bridging of the nitrogen atoms by the methylene groups, as in **12**, gives rise to a noncollapsible all-T structure of the macrocycle, with a well-defined hole. This is in contrast with the structure of **1**, which is flexible and can adopt to the environment, and similar to the effect of full protonation of the nitrogen atoms of **1**, stabilising all-T conformer. As would be expected, a negative ^1B_a Cotton effect is observed for **12**. This is fully confirmed by the calculated lowest-energy structure and CD spectrum of **12** (Figure 3).

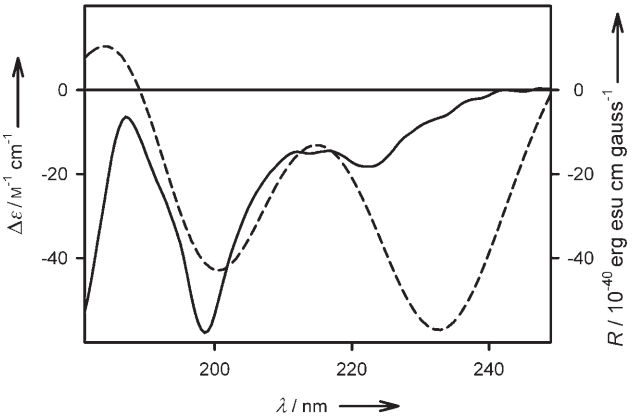

Figure 3. A comparison of experimentally measured (——) and ZINDO/S-calculated (-----) CD spectra of trianglamine **12**. Rotational strength *R* is calculated in the dipole-length representation.

In conclusion, CD spectra reflect changes of trianglamine ring conformation due to substitution and protonation of the nitrogen atoms.

Crystal structures of the inclusion complexes 1·PhF, 1·BzOMe, *ent*-1·AcOEt, 1·6HBr and 12·EtOH: To the best of our knowledge, this is the first report concerning the crystal structures of trianglamines, all of which crystallise with included solvent molecules. Unlike trianglimines, which contain rather rigid skeletons, trianglamines display various types of conformations in the solid state, in which the formal D_3 molecular symmetry is lost. The only exception is the fully protonated trianglamine **1**·6HBr, which maintains C_3 molecular symmetry in the solid state, whilst the molecule of **12**, formally asymmetric in the crystal, adopts a conformation that still approximates C_3 symmetry. The various types of conformation that these molecules display in their crystals are presented in Figure 4. Interestingly, the presence of three intramolecular hydrogen bonds of the N–H···N type does not prevent the macrocycle **1** from displaying flexibility. Partial rigidification of the trianglamine skeleton has also been achieved by $-CH_2-$ bridging (**12**) or by protonation (**1**·6HBr) of the nitrogen atoms and has also resulted in increases in the macrocycle symmetry.

Only T and G arrangements around the C–N bonds are observed, although in some cases close to the limiting values of 150 and 30°, respectively (Figure 4). Quite interestingly, for *R*,*R* enantiomers, the conformations around two neighbouring C–N bonds are described either by the T,T or T,G$^-$ sequences, indicating clear absence of G$^+$ conformers. The molecular conformation is stabilised by intramolecular hy-

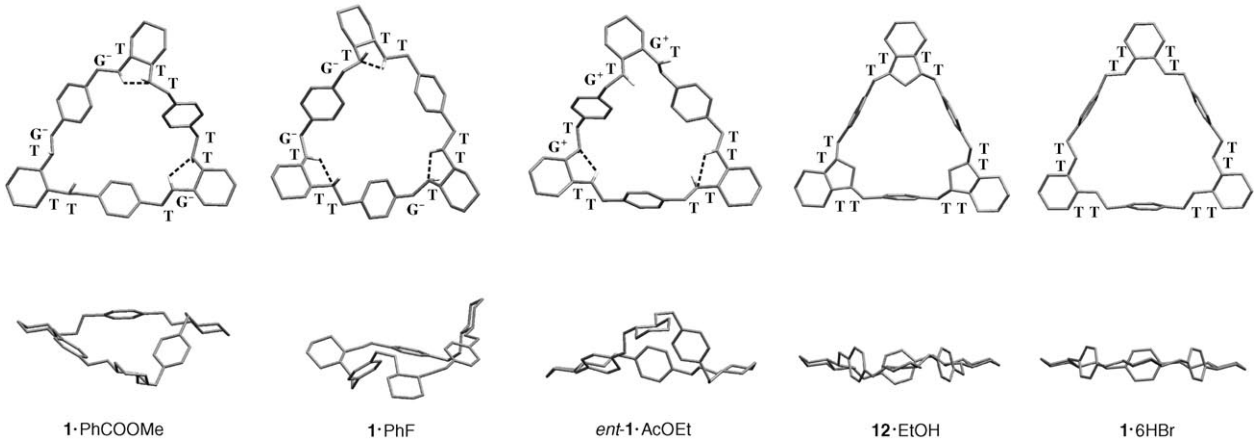

Figure 4. Conformers of trianglamines, viewed perpendicular and parallel to the main plane of the macrocycle. T and G designators describe conformation around the C–N bonds. Broken lines mark intramolecular hydrogen bonds.

drogen bonds of the N–H···N type, which involve three out of six amine hydrogen atoms.

The type of inclusion depends to a great extent on the structures of the hosts and the solvent molecules used for crystallisation (see Figures 5–7): aromatic guest molecules are accommodated in channels formed between layers of host **1** (Figure 5) while linear molecules are incorporated inside the molecular cavity (Figure 6).

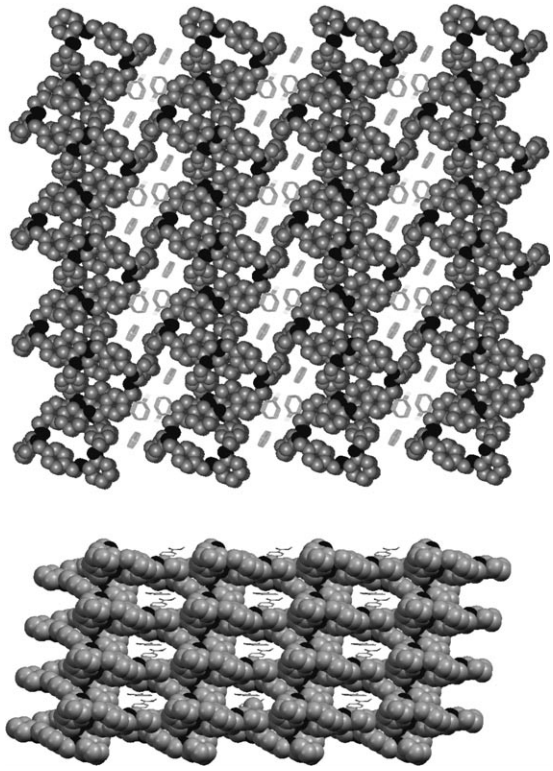

Figure 5. Illustration of one-dimensional channels in crystals of **1**·PhF (upper) and **1**·PhCOOMe (lower). Host atoms are shown as spheres of van der Waals radii. The channels formed between bilayers of the host molecules run nearly perpendicular (upper) or parallel (lower) to the macrocycle ring planes. The black spheres represent the N atoms.

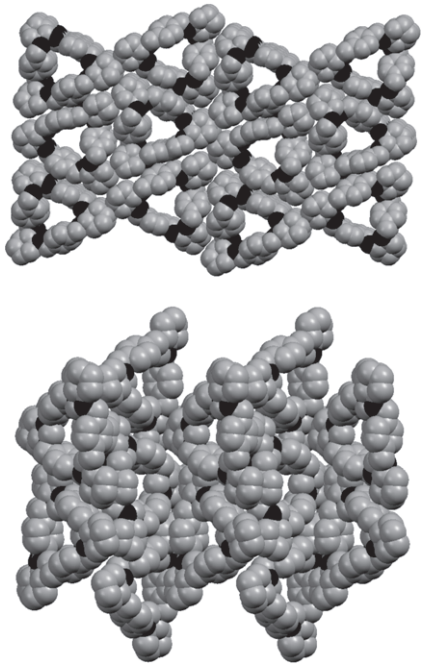

Figure 6. One-dimensional channels passing through the macrocyclic cavities in *ent*-**1**·AcOEt (upper), and **12**·EtOH (lower). Guests are omitted and the host atoms are shown as spheres of van der Waals radii. The black spheres represent the N atoms.

In **1**·PhF and **1**·PhCOOMe the trianglamine molecules are arranged in corrugated sheets, the neighbouring layers being shifted with respect to each other. Within each layer the molecules are held together by van der Waals forces, while between the consecutive layers there are hydrogen-bond interactions of the N–H···N type. In **1**·PhF, a two-dimensional host cavity formed between the host bilayers is closed by cyclohexane fragments, giving one-dimensional channels that are aligned nearly perpendicular to the mean plane of the macrocycle. The PhF molecules are accommodated in these channels in a host/guest ratio of 1:2. The included molecules are disordered (orientational disorder) and interact only

very weakly with the host molecule through N–H···F hydrogen bonds. The guest-accessible volume per unit cell amounts to 784 Å^3, which means that approximately 31.5% of the crystal volume is available for inclusion of guests. The term "porosity" (*P*) has been used in the literature to refer to this value.[27] Similarly, the trianglamine molecules in **1**·PhCOOMe are arranged in corrugated sheets, the two neighbouring layers being shifted with respect to each other. The solvent molecules are accommodated in channels between consecutive host bilayers. In this case, however, the solvent channels run nearly parallel to the macrocycle main plane and the host to guest ratio is 1:1. The guest-accessible volume per unit cell amounts to 544 Å^3, and the corresponding *P* value is 24.0%. Both crystals possess the same space group symmetry ($P2_1$) and similar ratios of unit-cell parameters, but the orientations of the host molecules with respect to the twofold screw axes are substantially different. The angles between the normals to the mean planes of the macrocycles and the *y* axes amount to 23.2 and 70.3° for **1**·PhF and **1**·PhCOOMe, respectively. This is in turn reflected in the values of the *a* and *b* cell constants, which are interchanged in the two crystals. Each methyl benzoate molecule is situated in-between two cyclohexane rings of the host, and is involved in C–H···π interactions with all axial C–H bonds of the two diaminocyclohexane molecules. The C–H···π interactions that involve aromatic rings and 1,2-diaminocyclohexane derivatives have recently been reported to be responsible for the formation of clathrates by the two types of molecules.[28]

Unlike aromatic guest molecules, the other guests are accommodated inside the channels passing through host molecules arranged in stacks (Figure 6). The repetition period in this direction is approximately 5 Å if the plane of the macrocycle is nearly perpendicular to the *x* direction, or amounts to approximately 9 Å if the macrocycles are inclined with respect to the *x* direction (Figure 6). The periodicities of the host and guest along the channel axis in the structures formed do not match. In *ent*-**1**·AcOEt the guest ethyl acetate molecules are disordered, as is one of the phenyl rings in the host molecule. This is a concerted host/guest disorder in which two equally occupied phenyl orientations either allow or prevent the presence of an ethyl acetate molecule in the macrocycle cavity. This dynamic behaviour illustrates extreme conformational flexibility in trianglamines and their tendency to avoid formation of large cavity-containing frameworks. The guest-accessible volume per unit cell when the phenyl ring closes the entrance to the macrocyclic cavity is only 232 Å^3 and the corresponding *P* value amounts to 5.8%, while the other orientation of the phenyl ring results in a solvent-accessible volume of 358 Å^3 and a *P* value of 9.1%.

Inclusion inside the macrocycle cavity is also observed in crystals of bridged trianglamine **12**, which crystallises with ethanol molecules in a host/guest ratio of 3:2. Unlike in the crystal structure of *ent*-**1**·AcOEt described above, however, in which the trianglamine planes are nearly perpendicular to the crystallographic *x* direction (the angle between the normal to the plane defined by the six nitrogen atoms in the macrocycle and the *x* direction amounts to 13.4°), the molecules in a stack in **12** are inclined with respect to the *x* axis, with the angle between the normal to the plane defined by the six nitrogen atoms in the macrocycle and the *x* direction amounting to 54.5°. Such an arrangement of molecules causes an increase of the unit translation along *x* from 5 to 9 Å and creates more space for the guest molecules aligned along the *x* axis. The guest-accessible volume per unit cell is approximately 625 Å^3, and the corresponding *P* value amounts to 14.4%.

The protonated trianglamine **1**·6HBr forms crystals of unusual symmetry (space group *P*321), which display both types of inclusion described above. The guest-accessible volume per unit cell is the largest in the studied crystals and amounts to 1133 Å^3, while the corresponding *P* value is 34.6%. The host molecules arrange in stacks along the [001] direction (Figure 7). The asymmetric unit consists of one third of a fully protonated trianglamine molecule lying around the threefold symmetry axis, with two bromide anions in general positions. This corresponds to a bromide/trianglamine ratio of 6:1. Within a macrocycle cavity, half of the statistically disordered Br_2 molecules are situated on a threefold symmetry axis. Water and methanol molecules, as well as Br^- anions, separate neighbouring triangles related by a unit translation along the *z* axis in a sandwich-type mode. The repeat period of these guest molecules, as well as Br_2 molecules situated in the molecular cavities, spans two unit cells in the [001] direction. In channels formed by six neighbouring host molecules, running along the direction of

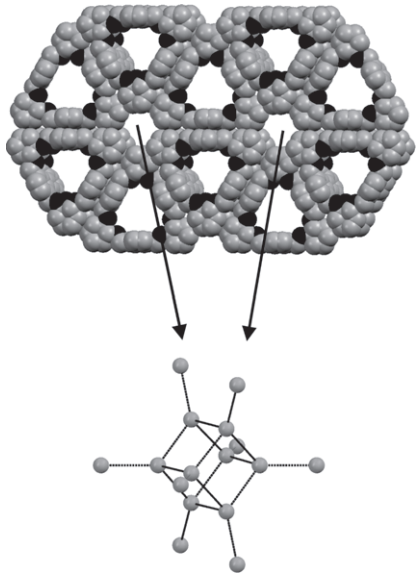

Figure 7. Illustration of one-dimensional channels formed inside and outside the macrocycle in **1**·6HBr. Four types of ion or molecule (Br^-, Br_2, MeOH and H_2O) are included within and between the macrocycles, which are arranged in stacks. The lattice channel is filled by highly unusual cubane-shaped clusters consisting of 16 water molecules. The black spheres represent the N atoms.

the threefold crystallographic z axis, one finds unusual cubical water clusters consisting of 16 water molecules hydrogen bonded to each other and to the bromide anions (Figure 7). The hydrogen-bonding pattern in this crystal structure is supplemented by N–H···Br^- and N–H···O types of interactions.

Conclusion

X-ray diffraction and CD studies, in conjunction with molecular modelling and calculations of the CD spectra, demonstrate that the macrocyclic skeletons of trianglamines **1** and **2** can assume a variety of low-energy conformations, describable in terms of T or G^- torsion angles around the C–N bonds. On the other hand, structures of the fully protonated **1** and the free base **12** appear to be conformationally restricted to all-T arrangements of the torsion angles around the C–N bonds. The crystal structures of hexamines differ significantly as a result of inclusion of various guests, solvent molecules and counteranions, and this can be ascribed to the facile formation of interpenetrated structures preventing formation of large cavities. The range of molecular conformations observed in the solid state is not only a demonstration of the substantial conformational flexibility of trianglamine **1**, but also of a tendency, in the absence of guest molecules, to reduce the inner cavity of the macrocycle as much as possible. The ability to include guest molecules in the crystal is strongly reduced in the case of N-alkylated derivatives **2**–**11** and is again demonstrated in the case of the methylene-bridged macrocycle **12**. In addition, our results indicate that supramolecular interactions involving macrocycle **1** do not follow a simple lock-and-key principle.

Shape complementarity of the components of inclusion complexes is the subject of current extensive studies. It was recently reported that benzene-1,3,5-tricarboxylic acid interacts more strongly with **1** in solution than its 1,2,3- and 1,2,4-isomers do.[21] However, we were not able to obtain any crystalline inclusion complexes by cocrystallisation of **1** with numerous aromatic carboxylic acid guest molecules, including benzene-1,3,5-tricarboxylic acid. It appears that, within the constraints of our conformational analysis of **1** and its inclusion complexes, the inner cavity of trianglamine **1** is not large enough to accommodate any trisubstituted benzene derivative. In fact, in no case studied by us could any aromatic guest molecule be found located inside the cavity of the macrocycle in the trianglamine crystalline inclusion complexes. We also note that, in view of the results of our study, macrocycle **1** cannot be considered rigid, as claimed previously.[22]

Further work on applications of trianglamines **1**–**12** in organic synthesis and supramolecular chemistry is in progress.

Experimental Section

Improved one-step synthesis of trianglamine 1: A mixture of (*R*,*R*)-1,2-diaminocyclohexane (*R*,*R*)-tartrate salt (5.28 g, 20 mmol), terephthalaldehyde (2.68 g, 20 mmol), methanol (200 mL) and triethylamine (7.0 mL, 50 mmol) was stirred overnight (the reagents dissolved and a precipitate of the product was formed). The mixture was cooled in an ice bath and sodium borohydride (2.28 g, 60 mmol) was added over one hour. After the system had been stirred for a further three hours at room temperature, the solvents were removed in vacuo and the residue was extracted with dichloromethane and aqueous sodium carbonate (5%). The organic solution was dried over magnesium sulfate, evaporated and dried in vacuo at 70°C for three hours. Trianglamine **1** was obtained in a yield of 4.1 g (96.5%). M.p. 154–156°C; $[\alpha]_D^{20} = -104$ (c = 1.3 in $CHCl_3$); ^{1}H NMR (300 MHz, $CDCl_3$, 20°C, TMS): δ = 1.03 (m, 2H; CH_2), 1.24 (m, 2H; CH_2), 1.74 (m, 2H; CH_2), 1.86 (br s, 2H; NH), 2.25 (m, 4H; CH_2), 3.62 (d, ^3J(H,H) = 12.9 Hz, 2H; $ArCH_2$), 3.92 (d, ^3J(H,H) = 12.9 Hz, 2H; $ArCH_2$), 7.29 ppm (s, 4H; Ar).

The product can be crystallised from ethyl acetate, but for further syntheses it was used as obtained. Crystallisation from aromatic solvents (or from mixtures of aromatic compounds and ethyl acetate) resulted in the formation of crystalline molecular complexes of varying stoichiometry. These complexes have characteristic melting points (Table 3). In many cases the complexes melt below 100°C and then solidify and melt again at approximately 155°C. These complexes are of lower stability and they slowly lose solvent molecules at room temperature. Some complexes (e.g., those with dioxane or pyridine) have high melting points and are of higher stability.

Table 3. Melting points of inclusion complexes of trianglamine **1** with aromatic guest molecules.

Guest (mole equivalent by ^{1}H NMR)	M.p. [°C]
fluorobenzene (2.0)	115–125
benzene (1.0)	96–99
toluene (1.0)	95–100
chlorobenzene (1.0)	96–103
phenol (1.0)	118–126
anisole (0.7)	94–100
nitrobenzene (0.7)	80–90
methyl benzoate (0.7)	132–135, 200–203
m-xylene (0.7)	107–112
1,3-dichlorobenzene (0.7)	104–108
1,3-dinitrobenzene (0.7)	144–159
mesitylene (0.9)	115–130, 185–194
1,3,5-trihydroxybenzene (0.5)	106–120
1,3,5-trimethoxybenzene (0.9)	112–115
trimethyl benzene-1,3,5-tricarboxylate (0.7)	103–110
hexafluorobenzene (–)	94–98
hexachlorobenzene (–)	134–140, 185–210
pyridine (0.5)	193–196

The hexahydrobromide of **1** was crystallised from water/methanol, m.p. 294–300°C (ref. [22]: m.p. 296–298°C).

Rac-**1** was obtained by crystallising equal amounts of (*R*,*R*)-**1** and (*S*,*S*)-**1** together; m.p. 174–177°C (from ethyl acetate). From the difference of the melting points of the racemate and the enantiomer (ca. 20°C) it appears that **1** crystallises as a racemic compound.

Hexa(*N*-methyl) derivative 2: A solution of trianglamine **1** (648 mg, 1 mmol) in a mixture of aqueous formaldehyde (36%, 2 mL) and formic acid (10 mL) was heated at reflux for 6 h. The solvents were evaporated and the residue was extracted with saturated aqueous $NaHCO_3$ and CH_2Cl_2. The organic extracts were evaporated to give the crude product (655 mg), which was crystallised from ethanol/hexane. The yield of **2** was 260 mg (71%). M.p. 182–186°C (after recrystallisation from acetone m.p.

187–190 °C); ^{1}H NMR (300 MHz, $CDCl_3$, 20 °C, TMS): δ = 1.18 (m, 2H; CH_2), 1.31 (m, 2H; CH_2), 1.77 (m, 2H; CH_2), 1.97 (m, 2H; CH_2), 2.19 (s, 6H; CH_3), 2.74 (m, 2H; CH_2), 3.74 (m, 4H; $ArCH_2$), 7.38 ppm (s, 4H, Ar); ^{13}C NMR (75 MHz, $CDCl_3$, 20 °C, TMS): δ = 26.0, 26.4, 35.9, 58.7, 65.0, 128.5, 139.2 ppm; EI MS: *m/z* (%): 732.7 (100) $[M]^+$.

General procedure for the synthesis of hexakis(*N*-alkylated) derivatives 3–6 and 8–11: A solution of trianglamine **1** (162 mg, 0.25 mol) and the corresponding bromide RBr (2 mmol; in the case of **4** a commercial 80% solution of propargyl bromide in toluene was used) in acetonitrile (5 mL) was heated at reflux with powdered K_2CO_3 (415 mg, 3 mmol) for 4 h. The solvent was evaporated and the residue was dissolved in CH_2Cl_2 and extracted with aqueous Na_2CO_3 (5%). The organic phase was dried over $MgSO_4$ and evaporated, and the crude product was purified by column chromatography on silica gel (solvent CH_2Cl_2 or CH_2Cl_2/AcOEt (19:1)).

Compound 3: Yield: 155 mg (70%); glass; ^{1}H NMR (300 MHz, $CDCl_3$, 20 °C, TMS): δ = 1.08 (m, 4H; CH_2), 1.70 (m, 2H; CH_2), 1.97 (m, 2H; CH_2), 2.71 (m, 2H; CHN), 2.94 (dd, ^3J(H,H) = 8.0, 14.0 Hz, 2H; CH), 3.29 (m, 4H; CH_2Ar), 3.73 (d, ^3J(H,H) = 13.4 Hz, 2H; CH_2Ar), 4.98 (d, ^3J(H,H) = 9.8 Hz, 2H; CH), 5.08 (d, ^3J(H,H) = 17.0 Hz, 2H; CH), 5.84 (m, 2H; CH), 7.26 ppm (s, 4H; Ar); ^{13}C NMR (75 MHz, $CDCl_3$, 20 °C, TMS): δ = 25.8, 26.1, 53.0, 53.2, 59.4, 115.8, 128.7, 138.4, 139.0 ppm; ESI MS: *m/z* (%): 890 (100) $[M+H]^+$.

Compound 4: Yield: 98 mg (45%); glass; ^{1}H NMR (300 MHz, $CDCl_3$, 20 °C, TMS): δ = 1.15 (m, 2H; CH_2), 1.40 (m, 2H; CH_2), 1.75 (m, 2H; CH_2), 2.16 (m, 2H; CH_2), 2.17 (s, 2H; CH), 2.92 (m, 2H; CHN), 3.39 (m, 4H; CH_2), 3.54 (d, ^3J(H,H) = 13.2 Hz, 2H; CH_2Ar), 3.88 (d, ^3J(H,H) = 13.2 Hz, 2H; CH_2Ar), 7.28 ppm (s, 4H; Ar); ^{13}C NMR (75 MHz, $CDCl_3$, 20 °C, TMS): δ = 26.1, 27.0, 38.1, 53.2, 61.7, 71.8, 82.7, 128.7, 138.2 ppm; IR (KBr): $\tilde{\nu}$ = 3299 (≡C–H), 2110 cm^{-1} (C≡C); ESI MS: *m/z* (%): 878 (100) $[M+H]^+$.

Compound 5: Yield: 165 mg (75%); glass; ^{1}H NMR (300 MHz, $CDCl_3$, 20 °C, TMS): δ = 1.24 (m, 2H; CH_2), 1.45 (m, 2H; CH_2), 1.86 (m, 2H; CH_2), 2.22 (m, 2H; CH_2), 2.85 (m, 2H; CHN), 3.41 (d, ^3J(H,H) = 17.6 Hz, 2H; CH_2CN), 3.54 (d, ^3J(H,H) = 17.6 Hz, 2H; CH_2CN), 3.77 (d, ^3J(H,H) = 13.2 Hz, 2H; CH_2Ar), 3.90 (d, ^3J(H,H) = 13.2 Hz, 2H; CH_2Ar), 7.27 ppm (s, 4H; Ar); ^{13}C NMR (75 MHz, $CDCl_3$, 20 °C, TMS): δ = 25.6, 26.5, 37.1, 54.1, 63.2, 117.7, 129.1, 136.9 ppm; IR (KBr): $\tilde{\nu}$ = 2228 cm^{-1} (C≡N); FAB MS: *m/z* (%): 883 (8) $[M+H]^+$.

Compound 6: Yield: 215 mg (74%); m.p. 57–61 °C; ^{1}H NMR (300 MHz, $CDCl_3$, 20 °C, TMS): δ = 1.11 (m, 4H; CH_2), 1.20 (t, ^3J(H,H) = 7.0 Hz, 6H; CH_3), 1.72 (m, 2H; CH_2), 2.05 (m, 2H; CH_2), 2.71 (m, 2H; CHN), 3.35 (d, ^3J(H,H) = 17.4 Hz, 2H; CH_2COOEt), 3.47 (d, ^3J(H,H) = 17.4 Hz, 2H; CH_2COOEt), 3.52 (d, ^3J(H,H) = 13.4 Hz, 2H; CH_2Ar), 3.87 (d, ^3J(H,H) = 13.4 Hz, 2H; CH_2Ar), 4.07 (q, ^3J(H,H) = 7.0 Hz, 4H; $COOCH_2$), 7.29 ppm (s, 4H; Ar); ^{13}C NMR (75 MHz, $CDCl_3$, 20 °C, TMS): δ = 14.3, 26.0, 27.2, 51.4, 53.8, 60.1, 61.3, 128.9, 138.1, 172.6 ppm; IR (KBr): $\tilde{\nu}$ = 1748 cm^{-1} (C=O); FAB MS: *m/z* (%): 1166 (24) $[M+H]^+$.

Compound 8: Yield: 210 mg (71%); m.p. 258–264 °C; ^{1}H NMR (300 MHz, $CDCl_3$, 20 °C, TMS): δ = 1.02 (m, 4H; CH_2), 1.69 (m, 2H; CH_2), 2.05 (m, 2H; CH_2), 2.69 (m, 2H; CHN), 3.33 (d, ^3J(H,H) = 13.6 Hz, 4H; CH_2Ar), 3.76 (m, 4H; CH_2Ar), 7.0–7.6 ppm (m, 14H; Ar); ^{13}C NMR (75 MHz, $CDCl_3$, 20 °C, TMS): δ = 25.0, 26.1, 53.0, 53.4, 58.4, 126.3, 127.5, 128.5, 129.0, 138.7, 140.5 ppm; FAB MS: *m/z* (%): 1189 (38) $[M+H]^+$.

Compound 9: Yield: 330 mg (79%); glass; ^{1}H NMR (300 MHz, $CDCl_3$, 20 °C, TMS): δ = 1.03 (m, 4H; CH_2), 1.70 (m, 2H; CH_2), 2.05 (m, 2H; CH_2), 2.63 (m, 2H; CHN), 3.31 (m, 4H; CH_2Ar), 3.69 (m, 4H; CH_2Ar), 7.0–7.6 ppm (m, 12H; Ar); ^{13}C NMR (75 MHz, $CDCl_3$, 20 °C, TMS): δ = 24.4, 25.9, 52.8, 58.4, 120.3, 128.6, 130.7, 131.0, 138.6, 139.5 ppm; FAB MS: *m/z* (%): 1666 (20) $[M+H]^+$.

Compound 10: Yield: 235 mg (70%); m.p. 175–185 °C; ^{1}H NMR (300 MHz, $CDCl_3$, 20 °C, TMS): δ = 1.07 (m, 4H; CH_2), 1.78 (m, 2H; CH_2), 2.10 (m, 2H; CH_2), 2.61 (m, 2H; CHN), 3.41 (m, 4H; CH_2Ar), 3.73 (m, 4H; CH_2Ar), 7.40 ppm (m, 12H; Ar); ^{13}C NMR (75 MHz, $CDCl_3$, 20 °C, TMS): δ = 24.5, 25.6, 53.2, 59.1, 110.5, 118.8, 128.6, 129.4, 131.7, 138.4, 146.1 ppm; IR (KBr): $\tilde{\nu}$ = 2226 cm^{-1} (C≡N); FAB MS: *m/z* (%): 1340 (7) $[M+H]^+$.

Compound 11: Yield: 250 mg (73%); glass; ^{1}H NMR (300 MHz, $CDCl_3$, 20 °C, TMS): δ = 1.02 (m, 4H; CH_2), 1.67 (m, 2H; CH_2), 2.04 (m, 2H; CH_2), 2.66 (m, 2H; CHN), 3.29 (m, 4H; CH_2Ar), 3.72 (m, 10H; CH_2Ar, OCH_3), 6.70 (m, 4H; Ar), 7.22 (m, 4H; Ar), 7.39 ppm (m, 4H; Ar); ^{13}C NMR (75 MHz, $CDCl_3$, 20 °C, TMS): δ = 24.9, 26.1, 52.7, 55.2, 58.1, 113.2, 128.5, 130.0, 132.6, 138.8, 158.1 ppm; FAB MS: *m/z* (%): 1370 (10) $[M+H]^+$.

Hexakis(*N*-hydroxyethyl) derivative 7: A solution of $LiAlH_4$ (60 mg) in THF (3 mL) was added to a solution of compound **5** (190 mg) in THF (3 mL) and the mixture was stirred for 3 h at room temperature. The reaction was quenched with ethyl acetate, followed by methanol. The solvents were evaporated and the mixture was extracted with CH_2Cl_2 and an aqueous solution of NaOH (1 N). The organic solution was dried ($MgSO_4$) and evaporated to give the glassy product **6** (150 mg, quantitative). ^{1}H NMR (300 MHz, $CDCl_3$, 20 °C, TMS): all signals are broad multiplets at room temperature; ^{13}C NMR (75 MHz, $CDCl_3$, 20 °C, TMS): δ = 23.6, 25.6, 49.9, 51.9, 54.7, 59.2, 129.8, 137.4 ppm (broad signals); IR (KBr): $\tilde{\nu}$ = 3385 cm^{-1} (O–H, broad); FAB MS: *m/z* (%): 914 (19) $[M+H]^+$.

Tris(*N,N'*-methylene) derivative 12: A solution of trianglamine **1** (324 mg, 0.5 mmol) and paraformaldehyde (180 mg, 6 mmol) in ethanol (10 mL) was heated at reflux for 5 h. After cooling, the crystalline product was filtered off and washed with ethanol. Yield: 265 mg (77%); m.p. 266–273 °C; ^{1}H NMR (300 MHz, $CDCl_3$, 20 °C, TMS): δ = 1.26 (m, 4H; CH_2), 1.82 (m, 2H; CH_2), 2.03 (m, 2H; CH_2), 2.28 (m, 2H; CHN), 3.16 (d, ^3J(H,H) = 14.0 Hz, 2H; CH_2Ar), 3.27 (s, 2H; CH_2), 4.07 (d, ^3J(H,H) = 14.0 Hz, 2H; CH_2Ar), 7.15 ppm (s, 4H; Ar); ^{13}C NMR (75 MHz, $CDCl_3$, 20 °C, TMS): δ = 24.6, 29.4, 57.5, 69.0, 77.1, 127.3, 137.8 ppm; EI MS: *m/z* (%): 683.7 (100) $[M]^+$.

The ^{1}H NMR spectrum of the crystal dissolved in $CDCl_3$ showed the presence of 0.66–0.80 mole equivalent of ethanol per mole of **12**. Product **12**, m.p. 290–293 °C (not crystallised) was also obtained in 60% yield by a general procedure for the synthesis of hexakis(*N*-alkylated) derivatives through the use of *N*-(chloromethyl)phthalimide (in this case the side product was phthalimide, m.p. 225–227 °C).

X-ray structure determinations

Compound 1·PhCOOMe: Compound **1**·PhCOOMe crystallised from methyl benzoate as an inclusion compound with the formula $C_{42}H_{60}N_6{\cdot}C_8H_8O_2$, M_r = 785.10, T = 170 K. Crystal system: monoclinic. Space group: $P2_1$. Unit-cell dimensions: a = 8.628(2), b = 15.043(3), c = 17.755(4) Å, β = 100.27(3)°; V = 2267.5(9) Å^3; Z = 2; ρ_{calcd} = 1.150 Mg m^{-3}; $Mo_{K\alpha}$ (λ = 0.71073, ω-scan); μ = 0.071 mm^{-1}. Final R value 0.0533 for 3283 observed reflections [$I > 2\sigma(I)$]. Crystal size: 0.4 × 0.4 × 0.08 mm^3. Data were collected with a KM4CCD kappa-geometry diffractometer[29] equipped with graphite monochromator. Theta range for data collection was 5.13 to 25.03° and the *hkl* ranges were −7/10, −17/17 and −21/21, respectively. Of the 11724 reflections collected, 4127 were unique (R_{int} = 0.0545) and 3283 were considered as observed with $I > 2\sigma(I)$. The intensity data were corrected for Lorentz-polarisation (Lp) effects. No absorption correction was applied.

Compound 1·PhF: Compound **1**·PhF crystallised from fluorobenzene as an inclusion compound with the formula $C_{42}H_{60}N_6{\cdot}2(C_6H_5F)$, M_r = 841.16, T = 294 K. Crystal system: monoclinic. Space group: $P2_1$. Unit-cell dimensions: a = 15.420(3), b = 8.592(2), c = 18.804(4) Å, β = 90.20(3)°; V = 2491.3(9) Å^3; Z = 2; ρ_{calcd} = 1.121 Mg m^{-3}; $Mo_{K\alpha}$ (λ = 0.71073, ω-scan); μ = 0.071 mm^{-1}. Final R value 0.076 for 4671 observed reflections [$I > 2\sigma(I)$]. Crystal size: 0.55 × 0.55 × 0.1 mm^3. Data were collected with a KM4CCD kappa-geometry diffractometer[29] equipped with graphite monochromator. Theta range for data collection was 5.10 to 25.03° and the *hkl* ranges were −11/18, −10/10 and −22/22, respectively. Of the 18701 reflections collected, 8557 were unique (R_{int} = 0.082) and 4671 were considered as observed with $I > 2\sigma(I)$. The intensity data were corrected for Lp effects. No absorption correction was applied. In order to account for the contribution of solvent molecules to the diffraction intensities, we have assumed the presence of orientational disorder by including two overlapping instances of the fluorobenzene molecules in the least-squares refinement. The disorder was modelled in the form of a major and minor component. Anisotropic displacement parameters were

applied only for the fluorine atoms constituting part of the major component. The other atoms constituting the solvent molecules were refined isotropically with constraints involving 1,2 and 1,3 distances.

Compound *ent*-1·AcOEt: Compound *ent*-**1**·AcOEt crystallised from ethyl acetate as an inclusion compound with the formula $C_{42}H_{60}N_6 \cdot 0.5(C_4H_8O_2)$, $M_r = 693.01$, $T = 170$ K. Crystal system: orthorhombic. Space group: $P2_12_12_1$. Unit-cell dimensions: $a = 5.189(1)$, $b = 3.926(5)$, $c = 31.607(6)$ Å; $V = 3924.1(1)$ Å^3; $Z = 4$; $\rho_{calcd} = 1.173$ Mg m^{-3}; $Mo_{K\alpha}$ ($\lambda = 0.71073$, ω-scan); $\mu = 0.071$ mm^{-1}. Final R value 0.063 for 3530 observed reflections [$I > 2\sigma(I)$]. Crystal size: $0.4 \times 0.3 \times 0.1$ mm^3. Data were collected with a KM4CCD kappa-geometry diffractometer[29] equipped with graphite monochromator. Theta range for data collection was 5.23 to 25.02° and the *hkl* ranges were −6/6, −28/27 and −37/27, respectively. Of the 20592 reflections collected, 6845 were unique ($R_{int} = 0.077$) and 3530 were considered as observed with $I > 2\sigma(I)$. The intensity data were corrected for Lp effects. No absorption correction was applied. Included chain molecules of ethyl acetate are disordered. The disorder was modelled under the assumption that the repeat period of these guest molecules spans two unit cells in the [100] direction.

Compound 12·EtOH: Compound **12**·EtOH crystallised from ethanol/chloroform as an inclusion compound with the formula $C_{45}H_{60}N_6 \cdot 0.67\,C_2H_5OH$, $M_r = 714.83$, $T = 295$ K. Crystal system: orthorhombic. Space group: $P2_12_12_1$. Unit-cell dimensions: $a = 9.288(2)$, $b = 18.162(4)$, $c = 25.796(5)$ Å; $V = 4351.5(16)$ Å^3; $Z = 4$; $\rho_{calcd} = 1.091$ Mg m^{-3}; $Mo_{K\alpha}$ ($\lambda = 0.71073$, ω-scan); $\mu = 0.065$ mm^{-1}. Final R value 0.077 for 4079 observed reflections [$I > 2\sigma(I)$]. Crystal size: $0.55 \times 0.40 \times 0.10$ mm^3. Data were collected with a KM4CCD kappa-geometry diffractometer[29] fitted with graphite monochromator. Theta range for data collection was 5.11 to 25.03° and the *hkl* ranges were −7/10, −21/21 and −30/30, respectively. Of the 22623 reflections collected, 7596 were unique ($R_{int} = 0.067$) and 4079 were considered as observed with $I > 2\sigma(I)$. The intensity data were corrected for Lp effects. No absorption correction was applied. Included ethanol molecules were refined isotropically with constraints imposed on 1,2 and 1,3 distances.

Compound 1·6HBr: Compound **1**·6HBr crystallised from methanol/water as an inclusion compound with the formula $C_{42}H_{66}N_6Br_6 \cdot 11.5\,H_2O \cdot 6\,CH_3OH \cdot 0.5\,Br_2$, $M_r = 1613.81$, $T = 150$ K. Crystal system: trigonal. Space group: $P321$. Unit-cell dimensions: $a = 22.478(3)$, $c = 7.476(1)$ Å; $V = 3271.3(8)$ Å^3; $Z = 2$; $\rho_{calcd} = 1.638$ Mg m^{-3}; $Mo_{K\alpha}$ ($\lambda = 0.71073$, ω-scan); $\mu = 4.360$ mm^{-1}. Final R value 0.061 for 2482 observed reflections [$I > 2\sigma(I)$]. Crystal size: $0.4 \times 0.4 \times 0.08$ mm^3. Data were collected with a KM4CCD kappa-geometry diffractometer[29] fitted with graphite monochromator. Theta range for data collection was 4.16 to 25.02° and the *hkl* ranges were −26/26, −18/26 and −8/8, respectively. Of the 22321 reflections collected, 3851 were unique ($R_{int} = 0.116$) and 2586 were considered as observed with $I > 2\sigma(I)$. The intensity data were corrected for Lp effects as well as absorption;[30] $T_{min} = 0.265$, $T_{max} = 0.706$.

Data reduction and analysis for all structures were carried out with CrysAlisRED.[31] The structures were solved by direct methods by use of SHELXS97,[32,33] and refined by the full-matrix least-squares techniques with SHELXL97.[34] Non-hydrogen atoms were refined anisotropically, except for the majority of solvent atoms, which were refined isotropically. The positions of all H atoms attached to carbon atoms were calculated geometrically (C–H = 0.96 Å). Because of disorder of the included solvent molecules not all H atoms contained in these molecules have been located. All H atoms were refined with a riding model and their isotropic displacement parameters were given a value 20% (or 30% in case of methyl hydrogen atoms) higher than the isotropic equivalent for the atom to which the H atoms were attached. The absolute structures of the crystals were assumed from the known absolute configurations of the (*R*,*R*)- or (*S*,*S*)-*trans*-1,2-diaminocyclohexane used in the syntheses. Mercury[35] and WebLab VieverPro[36] programs were used to prepare the drawings. The percentage of the volume accessible to guest molecules was estimated by use of the PLATON program.[37]

CCDC-272739 (**1**·PhCOOMe), -272740 (**1**·PhF), -272737 (*ent*-**1**·AcOEt), -272738 (**1**·6HBr) and -272741 (**12**·EtOH) contain the supplementary crystallographic data for this paper. These data can be obtained free of charge from the Cambridge Crystallographic Data Centre via www.ccdc.cam.ac.uk/data_request/cif.

Calculations: The conformational analyses were carried out for a representative set of six molecules: **1**, **1**·6H$^+$, **2**, **2**·3H$^+$, **2**·6H$^+$ and **12**. In all cases starting structures were those of the highest symmetry available for a given macrocycle. We first obtained the sets of conformers of the macrocycles accessible at ambient temperature from the results of conformational searches with use both of MM3 molecular mechanics force field and of CONFLEX software.[38] From these conformers we selected those with relative energies in the 0.0 to 10 kcal mol^{-1} range, and their structures were fully optimised with the aid of the AM1 Hamiltonian implemented in the Gaussian package.[39] In the cases of **2**·3H$^+$ and **2**·6H$^+$ all structures differing in absolute configuration at protonated nitrogen atoms were considered. We next selected optimized structures with relative energies ranging from 0.0 to 2.0 kcal mol^{-1}, and the percentage populations for all compounds were calculated on the basis of the ΔE values, with use of Boltzmann statistics and $T = 298$ K. For the sake of simplicity, only the lowest-energy conformers were used for further consideration. These constitute at least 80% of each of the entire conformer populations for each analysed structure: that is, **1** (91%), **1**·6H$^+$ (100%), **2** (82%), **2**·3H$^+$ (80%) and **12** (100%). It should be added that entropy difference between the conformers due to their symmetry may come into play for **2**·3H$^+$ (C_3 symmetry of the second-lowest energy conformer). Here the entropy of symmetry contribution is $-R\ln 3$, so the C_3 symmetry conformer is additionally stabilised by 0.65 kcal mol^{-1} at 298 K. This translates to a reduction of the population of the lowest-energy conformer of C_1 symmetry to 56%. In the cases of **1**·6H$^+$ and **12** (D_3 symmetry of the lowest-energy conformers) the entropy of symmetry contribution ($-R\ln 6$) further stabilises the lowest-energy conformers, already contributing over 99% to the equilibrium.

Finally, for all the lowest-energy conformers of **1**, **1**·6H$^+$, **2**, **2**·3H$^+$, and **12**, the rotational and oscillator strengths were calculated by use of the ZINDO/S method. The computed oscillator strengths and rotational strengths were converted into the UV and CD spectra with the assumption of Gaussian shape absorption curves, by the methodology described by Grimme et al.[40] No correction for the dielectric constant of the medium was implemented. In all calculated spectra the transition energies were underestimated (by ca. 20 nm) and were scaled by the factor of 0.92 to match the experimentally obtained UV maxima.

Acknowledgements

MK wishes to thank the Foundation for Polish Science (FNP) for support. All calculations were performed at the Poznan Supercomputing Center.

[1] F. Vögtle, G. Pawlitzki, U. Hahn in *Modern Cyclophane Chemistry* (Eds.: R. Gleiter, H. Hopf), Wiley-VCH, Weinheim, **2004**, Chapter 2.
[2] C. Grave, A. D. Schülter, *Eur. J. Org. Chem.* **2002**, 3075–3098.
[3] K. E. Krakowiak, R. M. Izatt, J. S. Bradshaw, *J. Heterocycl. Chem.* **2001**, *38*, 1239–1248.
[4] J. Gawronski, H. Kołbon, M. Kwit, A. Katrusiak, *J. Org. Chem.* **2000**, *65*, 5768–5773.
[5] M. Chadim, M. Buděšinsky, J. Hodačova, J. Zavada, P. C. Junk, *Tetrahedron: Asymmetry* **2001**, *12*, 127–133.
[6] N. Kuhnert, A. M. Lopez-Periago, *Tetrahedron Lett.* **2002**, *43*, 3329–3332.
[7] N. Kuhnert, G. M. Rossignolo, A. M. Lopez-Periago, *Org. Biomol. Chem.* **2003**, *1*, 1157–1170.
[8] N. Kuhnert, C. Straßnig, A. M. Lopez-Periago, *Tetrahedron: Asymmetry* **2002**, *13*, 123–128.
[9] M. Kwit, P. Skowronek, H. Kołbon, J. Gawronski, *Chirality* **2005**, *17*, S92–S100

[10] N. Kuhnert, N. Burzlaff, C. Patel, A. Lopez-Periago, *Org. Biomol. Chem.* **2005**, *3*, 1911—1921.
[11] N. Kuhnert, A. M. Lopez-Periago, G. M. Rossignolo, *Org. Biomol. Chem.* **2005**, *3*, 524–537.
[12] J. Gao, A. E. Martell, *Org. Biomol. Chem.* **2003**, *1*, 2801–2806.
[13] a) S. R. Korupoju, P. S. Zacharias, *Chem. Commun.* **1998**, 1267–1268; b) S. R. Korupoju, N. Mangayarkarasi, S. Ameerunisha, E. J. Valente, P. S. Zacharias, *J. Chem. Soc. Dalton Trans.* **2000**, 2845–2852.
[14] J. Gregolinski, J. Lisowski, T. Lis, *Org. Biomol. Chem.* **2005**, *3*, 3161–3166.
[15] M. Kwit, J. Gawronski, *Tetrahedron: Asymmetry* **2003**, *14*, 1303–1308.
[16] Z. Li, C. Jablonski, *Chem. Commun.* **1999**, 1531–1532.
[17] J. Gao, J. H. Reibenspies, R. A. Zingaro, F. R. Woolley, A. E. Martell, A. Clearfield, *Inorg. Chem.* **2005**, *44*, 232–241.
[18] a) S. Akine, T. Taniguchi, T. Nabeshima, *Tetrahedron Lett.* **2001**, *42*, 8861–8864; b) S. Akine, D. Hashimoto, T. Saiki, T. Nabeshima, *Tetrahedron Lett.* **2004**, *45*, 4225–4227.
[19] a) A. J. Gallant, M. J. MacLachlan, *Angew. Chem.* **2003**, *115*, 5465–5468; *Angew. Chem. Int. Ed.* **2003**, *42*, 5306–5310; b) A. J. Gallant, B. O. Patrick, M. J. MacLachlan, *J. Org. Chem.* **2004**, *69*, 8739–8744; c) C. Ma, A. Lo, A. Abdolmaleki, M. J. MacLachlan, *Org. Lett.* **2004**, *6*, 3841–3844.
[20] S. J. Rowan, D. G. Hamilton, P. A. Brady, J. K. M. Sanders, *J. Am. Chem. Soc.* **1997**, *119*, 2578–2579.
[21] J. Hodačova, M. Chadim, J. Zavada, J. Aguilar, E. Garcia-Espana, S. V. Luis, J. F. Miravet, *J. Org. Chem.* **2005**, *70*, 2042–2047.
[22] J. Gao, A. E. Martell, *Org. Biomol. Chem.* **2003**, *1*, 2795–2800.
[23] J. Gao, R. A. Zingaro, J. H. Reibenspies, A. E. Martell, *Org. Lett.* **2004**, *6*, 2453–2455.
[24] a) F. Galsbol, P. Steenbol, B. S. Sorensen, *Acta Chem. Scand.* **1972**, *26*, 3605–3611; b) J. F. Larrow, E. N. Jacobsen, Y. Gao, Y. Hong, X. Nie, C. M. Zepp, *J. Org. Chem.* **1994**, *59*, 1939–1942.
[25] a) M. Kwit, J. Gawronski, *Tetrahedron Lett.* **2003**, *44*, 8311–8314; b) M. Kwit, J. Gawronski, *Tetrahedron* **2003**, *59*, 9323–9331.
[26] Z. Y. Wang, E. K. Todd, X. S. Meng, J. P. Gao, *J. Am. Chem. Soc.* **2005**, *127*, 11552–11553.
[27] J.-H. Fournier, T. Maris, J. D. West, *J. Org. Chem.* **2004**, *69*, 1762–1775.
[28] E. Rafii, M. Giorgi, N. Vanthuyne, Ch. Roussel, *ARKIVOC* **2005**, (x), 86–94.
[29] CrystAlis CCD software, version 1.171, Oxford Diffraction, Oxfordshire (England), **2000**.
[30] User Manual, Xcalibur Series, Single Crystal Diffractometers, version 1.3, Oxford Diffraction, Oxfordshire (England), **2002**.
[31] CrystAlis RED software, version 1.171, Oxford Diffraction, Oxfordshire (England), **2000**.
[32] G. M. Sheldrick, *Acta Crystallogr. Sect. A* **1990**, *46*, 467–473.
[33] G. M. Sheldrick, SHELXS-97, Program for the Solution of Crystal Structure, University of Göttingen (Germany), **1997**.
[34] G. M. Sheldrick, SHELXL-97, Program for the Refinement of Crystal Structure, University of Göttingen (Germany), **1997**.
[35] a) I. J. Bruno, J. C. Cole, P. R. Edgington, M. K. Kessler, C. F. Macrae, P. McCabe, J. Pearson, R. Taylor, *Acta Crystallogr. Sect. B* **2002**, *58*, 389–397; b) R. Taylor, C. F. Macrae, *Acta Crystallogr. Sect. B* **2001**, *57*, 815–827.
[36] MSI. WebLab ViewerPro, Version 3.5, Molecular Simulation Inc., 9685 Scranton Road, San Diego, CA 92121 (USA), **1999**.
[37] A. L. Speak, *Acta Crystallogr. Sect. A* **1990**, *46*, 194–201.
[38] CAChe 5.0 WS Pro, Fujitsu Ltd., **2001**.
[39] Gaussian 03, Revision B.04, M. J. Frisch, G. W. Trucks, H. B. Schlegel, G. E. Scuseria, M. A. Robb, J. R. Cheeseman, J. A. Montgomery, Jr., T. Vreven, K. N. Kudin, J. C. Burant, J. M. Millam, S. S. Iyengar, J. Tomasi, V. Barone, B. Mennucci, M. Cossi, G. Scalmani, N. Rega, G. A. Petersson, H. Nakatsuji, M. Hada, M. Ehara, K. Toyota, R. Fukuda, J. Hasegawa, M. Ishida, T. Nakajima, Y. Honda, O. Kitao, H. Nakai, M. Klene, X. Li, J. E. Knox, H. P. Hratchian, J. B. Cross, V. Bakken, C. Adamo, J. Jaramillo, R. Gomperts, R. E. Stratmann, O. Yazyev, A. J. Austin, R. Cammi, C. Pomelli, J. W. Ochterski, P. Y. Ayala, K. Morokuma, G. A. Voth, P. Salvador, J. J. Dannenberg, V. G. Zakrzewski, S. Dapprich, A. D. Daniels, M. C. Strain, O. Farkas, D. K. Malick, A. D. Rabuck, K. Raghavachari, J. B. Foresman, J. V. Ortiz, Q. Cui, A. G. Baboul, S. Clifford, J. Cioslowski, B. B. Stefanov, G. Liu, A. Liashenko, P. Piskorz, I. Komaromi, R. L. Martin, D. J. Fox, T. Keith, M. A. Al-Laham, C. Y. Peng, A. Nanayakkara, M. Challacombe, P. M. W. Gill, B. Johnson, W. Chen, M. W. Wong, C. Gonzalez, J. A. Pople, Gaussian, Inc., Pittsburgh PA, **2003**.
[40] C. Diedrich, S. Grimme, *J. Phys. Chem. A* **2003**, *107*, 2524–2539.

Received: July 26, 2005
Published online: November 30, 2005

